JOURNAL OF VIROLOGY, Feb. 1988, p. 534–544
0022-538X/88/020534-11$02.00/0

Vol. 62, No. 2

The Avian Erythroblastosis Virus *erbA* Oncogene Encodes a DNA-Binding Protein Exhibiting Distinct Nuclear and Cytoplasmic Subcellular Localizations

PHILIP BOUCHER,[1] ANN KONING,[2] AND MARTIN L. PRIVALSKY[3]*

Departments of Biochemistry/Biophysics,[1] Genetics,[2] and Bacteriology,[3] University of California, Davis, California 95616

Received 24 August 1987/Accepted 16 October 1987

The protein product of the v-*erbA* oncogene of avian erythroblastosis virus was analyzed by use of site-specific antisera. The v-*erbA* protein was found to exist in distinct nuclear and cytoplasmic forms. Both nuclear and cytoplasmic species of the v-*erbA* protein were capable of binding to DNA, a property predicted based on the structural relatedness the v-*erbA* polypeptide shares with the thyroid and steroid hormone receptors. A mutation within the v-*erbA* coding region which inhibited DNA binding and nuclear localization also inhibited the ability of the v-*erbA* protein to potentiate erythroid transformation, consistent with a model of the v-*erbA* protein as a transcriptional regulator.

The avian erythroblastosis virus (AEV) possesses two distinct loci that mediate oncogenic transformation by this retrovirus, v-*erbA* and v-*erbB* (2, 27, 30, 32, 38, 39, 43, 51, 58). The v-*erbB* gene is both necessary and sufficient for oncogenesis and encodes a tyrosine-specific protein kinase (17, 20, 26, 31, 41, 50, 57). In contrast, the v-*erbA* gene is not capable of autonomous oncogenic transformation but instead possesses the ability to potentiate erythroid transformation by a variety of other oncogenes, including v-*erbB* (17, 29, 49). v-*erbA* appears to act by blocking transformed erythroid cells in an immature differentiation state (7, 17, 22, 29). Thus, erythroid cell progenitors transformed by the v-*erbB* oncogene alone tend to spontaneously differentiate into more mature erythroblasts, reticulocytes, and terminally differentiated erythrocytes. In contrast, erythroid cells transformed by v-*erbB* in the presence of v-*erbA* remain tightly blocked in a relatively undifferentiated state and retain a high proliferative capacity (8, 9, 17, 19, 23, 29, 45). The v-*erbA* oncogene has also been reported to have subtle effects on the phenotype of fibroblasts (18).

With increasing frequency, loci first identified in the guise of retroviral oncogenes have subsequently been proven to be transduced copies of host genes (termed c- or proto-oncogenes) involved in regulation of normal cellular growth and proliferation. The proto-*erbA* gene, one of a multigene family in mammals, appears to encode a thyroid hormone receptor (T3/T4 thyronine receptor) or an extremely closely related polypeptide (46, 55). The v- (and c-) *erbA* proteins also demonstrate a more distant structural relatedness to the steroid hormone receptors (11, 24, 25, 54). Comparison of the amino acid sequences of the v-*erbA* protein with those of the steroid hormone receptors permits several potential functional domains to be ascertained, including a cysteine-rich, "zinc-finger" motif which, in the steroid receptors, is thought to be involved in DNA binding, a lysine-arginine-rich domain, and a C-terminal domain which in the thyroid and steroid hormone receptors is the hormone-binding region (11, 24, 25, 46, 54, 55) (Fig. 1). Unlike the c-*erbA* progenitor, however, the viral v-*erbA* protein appears to have lost the ability to bind thyroid hormone (46).

Both steroid and thyroid hormone receptors function at the level of transcription: hormone binding to the receptor molecule activates its ability to interact with specific DNA enhancerlike elements, stimulating or suppressing the transcription of nearby genes (for reviews, see references 37, 53, and 56). The structural similarity of the v-*erbA* protein to thyroid and steroid hormone receptors suggests the viral oncogene product operates through a similar transcriptional regulatory mechanism. However, many key features of this model have yet to be confirmed or rely on published data which remain controversial. For example, early experiments indicated the v-*erbA* protein was, in fact, a cytoplasmic polypeptide, leading to the suggestion v-*erbA* might act in oncogenesis not by mimicking the action of c-*erbA* but by interfering with the normal c-*erbA* function (1, 10, 35). In contrast, a more recent report suggests that the v-*erbA* polypeptide is actually (and exclusively) a nuclear protein (46), in better agreement with a mechanism of action analogous to that of the T3/T4 receptor progenitor. No attempt has been made to reconcile these apparently contradictory results.

To resolve these questions and to better elucidate the possible mechanisms of action of the v-*erbA* gene product, we initiated a study of the biochemical properties of both wild-type and mutant forms of the v-*erbA* polypeptide. Our results demonstrate that the v-*erbA* protein exists in both nuclear and cytoplasmic fractions, that the v-*erbA* protein found in both fractions is capable of binding to DNA, and that a site-specific mutation in the v-*erbA* gene within a lysine-arginine codon-rich domain inhibits the nuclear localization, DNA binding, and biological activity of the encoded polypeptide. These properties are consistent with models which propose that the v-*erbA* protein functions in transformed cells as a modulator of host cell gene transcription, mimicking the action of a constitutively "on" hormone receptor (46, 55).

MATERIALS AND METHODS

Cells and viruses. Cells and viruses were obtained and propagated as previously described (36, 42). The 366 mutation was created by insertion of an *Hpa*I oligonucleotide linker into the AEV molecularly cloned genome at an *Alu*I site 366 base pairs downstream from the start of the v-*erbA*-specific sequence (14, 36, 46, 50). Fibroblasts infected by the

* Corresponding author.

Rous-associated virus-1 (RAV-1) helper virus alone, wild-type AEV, or the AEV 366 mutant were obtained by transfecting chicken embryo secondary cells with appropriate molecular clones of the AEV and RAV genomes (36, 50).

Immunological reagents. Synthetic oligopeptides were purchased from OCS Laboratories, Denton, Tex. Three oligopeptide sequences were chosen for use as antigens by scanning the elucidated v-*erbA* protein sequence for strongly hydrophilic domains or domains rich in prolines or both (14, 46, 52): peptide 1 (H_2N-KSLQHRPSPSAEE-COOH; representing v-*erbA* codons 138 to 150), peptide 2 (H_2N-RYDPE SETLTLSGE-COOH; representing v-*erbA* codons 252 to 265), and peptide 3 (H_2N-CPTELPPRRC-COOH; representing v-*erbA* codons 378 to 387). Conjugation of peptides to keyhole limpet hemocyanin (Sigma Chemical Co., St. Louis, Mo.) was performed using either 1-ethyl-3-(3-dimethylaminopropyl)carbodiimide (EDC) or glutaraldehyde as the cross-linking reagent (47). Immunization of rabbits was performed as previously described; antibody production was monitored by enzyme-linked immunosorbent assay (48). Generally the most reactive serum was obtained after the third or fourth boost. Rabbit anti-*gag* protein serum was generously donated by H. Oppermann and J. M. Bishop.

Radioisotopic labeling of cells. Cells were metabolically radiolabeled with [^{35}S]methionine, as previously described (42), in RPMI medium lacking unlabeled methionine (GIBCO Laboratories, Grand Island, N.Y.). Cells were labeled with [^{32}P]phosphate as follows: cell cultures were washed twice with RPMI medium lacking P_i and then preincubated in the same medium for 2 h at 39°C. Next, [^{32}P]phosphate (carrier free; 200 to 1,000 μCi/10^6 cells) was added to the culture medium, and the cells were incubated for an additional 4 to 6 h before being harvested and subjected to immunoprecipitation.

Cell lysis and subcellular fractionation. Several methods and conditions of cell lysis and fractionation were tested on radiolabeled cells. The optimized protocol was as follows: approximately 5×10^6 to 1×10^7 AEV-transformed cells were washed twice in ice-cold phosphate-buffered saline (PBS) and subsequently lysed by incubation in 0.25 ml of PTMA buffer (15 mM potassium phosphate [pH 7.5], 0.5% Triton X-100, 1.1 mM $MgCl_2$, 1 mg of bovine serum albumin per ml) for 15 min on ice. AEV-erythroid cells were processed as a suspension, whereas AEV-fibroblasts were usually lysed directly on the culture plate. All subsequent manipulations were carried out at 0°C. Nuclei were pelleted by a 5-min centrifugation at 1,000 × *g*, washed once in 0.25 ml of PTMA, and repelleted as before. The two 1,000 × *g* supernatants, representing the cytoplasm-plus-membrane fraction, were pooled and adjusted to 0.5 M NaCl. The final 1,000 × *g* pellet (nuclear fraction) was resuspended in 0.5 ml of PTMA buffer, adjusted to 0.5 M NaCl, and sonicated for two 15-s bursts at a setting of 5 with a Heat Systems sonicator with microtip. Insoluble debris was removed by a 2-min centrifugation at 10,000 × *g* before immunoprecipitation.

Immunoprecipitation analysis. All immunoprecipitations were carried out at 0 to 4°C using a 20- to 40-fold dilution of antiserum as described previously (42). This usually represented an antibody excess; the competition assay for which results are shown in Fig. 2 was performed in antigen excess. Immunoprecipitates were analyzed by electrophoresis on 8% sodium dodecyl sulfate (SDS)-polyacrylamide gels and visualized by fluorography (42).

DNA-binding assays. The ability of the v-*erbA* protein to bind to DNA was tested as described for the thyroid hormone receptor (33), with minor modifications. AEV-infected cells (approximately 2×10^6 cells per assay) were radiolabeled with [^{35}S]methionine for 2 h, washed in 10 mM Tris chloride (pH 7.5)–150 mM NaCl, and suspended in 100 μl of 10 mM Tris chloride (pH 7.6)–100 mM NaCl–1% Nonidet P-40–1 mg of bovine serum albumin per ml. The cells were then either immediately sonicated, generating a whole-cell extract, or first separated into nuclear and cytoplasm-plus-membrane fractions as described above. Cell extracts were centrifuged at 10,000 × *g* for 1 min to remove debris before being added to the DNA-cellulose binding reaction mixture (see below).

Double-stranded DNA-cellulose (Sigma; 4.3 mg of calf thymus DNA per g of cellulose) was swollen (33) and washed several times in TGED buffer (20 mM Tris chloride [pH 8.2], 5% glycerol, 1 mM EDTA, 0.1 mM dithiothreitol) before use. The DNA-binding reaction was begun by mixing 100 μl of cell lysate, 200 μl of 2× binding buffer (40 mM Tris chloride [pH 8.2], 20% glycerol, 0.2 M NaCl, 0.2 mM dithiothreitol), 100 μl of water (or, for competition experiments, a 10-mg/ml solution of sonicated DNA), and 100 μl of a 10% slurry of DNA-cellulose (in TGED buffer). The mixtures were then gently rocked at 4°C for 1 h. The DNA-cellulose was subsequently pelleted (10 s in a Microfuge [Beckman Instruments, Inc., Fullerton, Calif.]), and the supernatant (representing the unbound fraction) was saved. The DNA-cellulose pellet was washed three times with 1× binding buffer, and proteins bound to the DNA matrix were eluted in a final 500-μl wash with 1× binding buffer containing 0.5 M KCl. All samples were adjusted to 0.5 M KCl–1% Nonidet P-40–1 mg of bovine serum albumin per ml and subjected to analysis by immunoprecipitation and SDS-polyacrylamide gel electrophoresis (PAGE).

Immunofluorescence microscopy. Infected fibroblasts were plated directly on top of microscope cover slips in preparation for immunofluorescence microscopy (47). After incubation in growth medium overnight at 39°C, the cells on the cover slips were washed twice with PBS and fixed for 20 min in 3.6% *p*-formaldehyde in PBS at 4°C. The cover slips were again washed in PBS and then sequentially treated with 50% acetone–50% water for 3 min (0°C), 100% acetone for 5 min (−20°C), and 50% acetone–50% water for 3 min (0°C). Subsequent steps were performed at room temperature. After several additional washes with PBS, the cover slips were incubated in 10% fetal bovine serum–PBS for 30 min to quench nonspecific protein adsorption. The cells were washed again in PBS and then incubated in a 40-fold dilution of the primary antiserum in 10% fetal bovine serum–PBS for 30 min. The cover slips were then repeatedly washed in PBS before incubation with a 40-fold dilution of rhodamine-conjugated goat anti-rabbit immunoglobulin G (Organon Teknika, Malvern, Pa.) in 10% fetal calf serum–PBS for 30 min. After an extensive final washing in PBS, the cover slips were examined by epifluorescence under a Nikon Microphot-FX microscope.

RESULTS

Development of a series of site-specific antisera directed against the *v-erbA* protein. The viral v-*erbA* protein is synthesized in the form of a 75,000-molecular-weight *gag-erbA* fusion polypeptide ($p75^{gag\text{-}erbA}$ [2, 27, 30, 32, 38, 43, 51, 58]). Most previous research on v-*erbA* has made use of *gag*-directed sera to detect this fusion polypeptide, although some work using *erbA*-reactive, tumor-bearing animal sera has also been reported (6, 26, 46). We chose to develop a

series of site-specific antisera directed against defined domains of the v-*erbA*-specific sequence itself. These defined immunological reagents would enable us to detect any processed forms of the v-*erbA* protein that might lack *gag* determinants and would permit us to perform immunofluorescence and immunoprecipitation studies under circumstances in which helper virus-encoded *gag* proteins might otherwise interfere with the analysis.

Three different oligopeptides were chemically synthesized to correspond to three distinct regions of the predicted v-*erbA* amino acid sequence (Fig. 1), and each peptide, coupled to keyhole limpet hemocyanin, was inoculated into rabbits (14, 47). Each of the resulting sera demonstrated strong enzyme-linked immunosorbent assay titers against the corresponding peptide antigen, and all three sera immunoprecipitated a 75,000-molecular-weight polypeptide from both AEV-infected fibroblasts and erythroid cells (the results of a representative immunoprecipitation using anti-peptide 2 sera are shown in Fig. 2, lane 2). The 75,000-molecular-weight protein recognized by our peptide-directed antisera was identical, by partial proteolysis mapping, to the $p75^{gag\text{-}erbA}$ protein previously detected by *gag*-directed sera (Fig. 2, lane 5, and data not shown). Preimmune sera failed to precipitate the $p75^{gag\text{-}erbA}$ polypeptide (lane 1), and the p75 protein was not detected in cells infected by a RAV-1 helper virus alone (data not shown). The specificity of our different antisera was further confirmed by use of the oligopeptide antigens in competition experiments. For example, immunoprecipitation of $p75^{gag\text{-}erbA}$ by sera raised against oligopeptide 2 was strongly inhibited by inclusion of an excess of oligopeptide 2 in the precipitation reaction mixture but was not significantly inhibited by peptide 1 or by keyhole limpet hemocyanin (Fig. 2, lanes 3 and 4, and data not shown).

Unexpectedly, antisera directed against the most C-terminal sequence, peptide 3, possessed strong enzyme-linked immunosorbent assay titers against the peptide 3 antigen but a relatively weak ability to immunoprecipitate the native $p75^{gag\text{-}erbA}$ protein (data not shown). Sera from only two of the eight rabbits immunized with this peptide were reactive with the native protein. Subsequently we learned that the published v-*erbA* DNA sequence (14) upon which we based this oligopeptide was in error and that only the first 5 of the 10 amino acids in our peptide 3 antigen are actually represented in the authentic v-*erbA* protein (46). In contrast, both peptides 1 and 2 accurately represent sequences found in the authentic v-*erbA* protein, as confirmed by sequence analysis in two independent laboratories (14, 46). Unless otherwise indicated, the data presented in this manuscript were obtained by use of the anti-peptide 2 sera. Parallel experiments using anti-peptide 1 or anti-*gag* protein sera were usually performed to confirm or extend these results and are discussed.

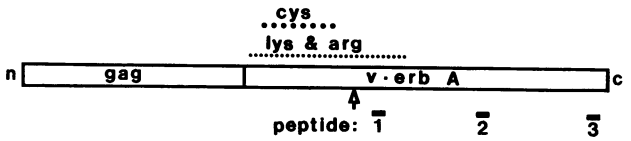

FIG. 1. Schematic of the p75 *gag*-v-*erbA* protein. The boundaries of *gag*- and v-*erbA*-specific domains are depicted, as are the locations of the three sequences used to raise oligopeptide-directed antisera (see the text). The location of the 366 insertion mutation (arrow) is also shown. The approximate boundaries of cysteine-rich (cys) and lysine-arginine-rich (lys & arg) motifs, thought to represent possible DNA-binding domains, are indicated.

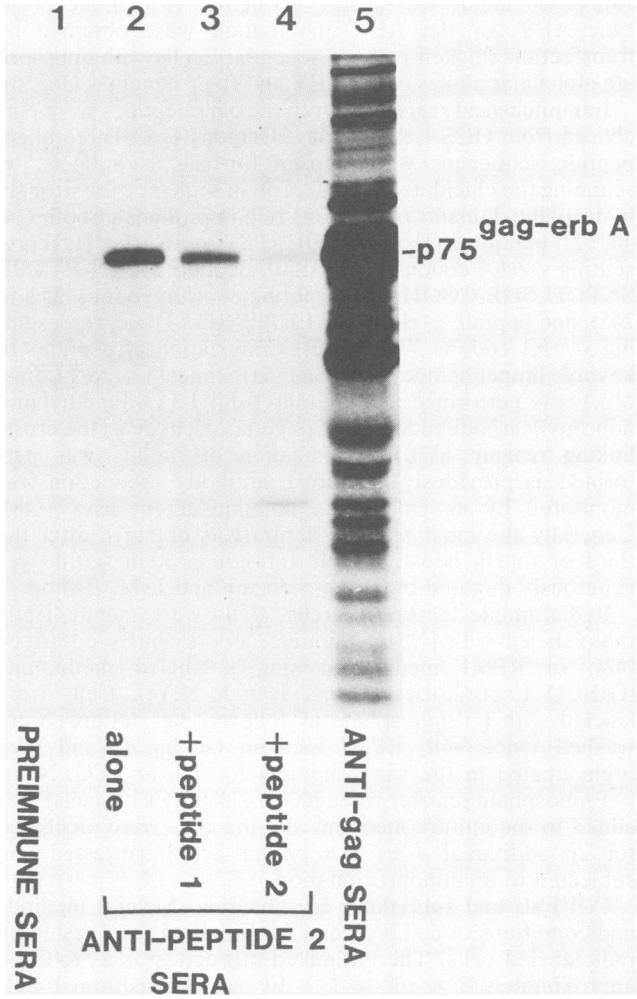

FIG. 2. Specificity of anti-v-*erbA* peptide 2 sera. AEV-transformed erythroid cells were metabolically radiolabeled with [^{35}S]methionine for 2 h and lysed, and the lysates were immunoprecipitated with various antisera, as described in the text. The immunoprecipitated proteins were analyzed by SDS-PAGE and visualized by fluorography. Shown are the proteins immunoprecipitated by 5 μl each of preimmune sera (lane 1), anti-peptide 2 sera (lane 2), anti-peptide 2 sera in the presence of an excess (2 μg/μl) of peptide 1 (lane 3), anti-peptide 2 sera in the presence of an excess (2 μg/μl) of peptide 2 (lane 4), and anti-*gag*-directed sera (lane 5). The slight nonspecific inhibition of anti-peptide 2 sera by peptide 1 (lane 3) was detected only at these relatively high competing-peptide concentrations. Molecular weight markers, run in an adjacent lane, are not shown. The position of the 75,000-molecular-weight (p75) *gag*-v-*erbA* protein is indicated.

The p75 *gag*-v-*erbA* protein was found in both cytoplasmic and nuclear fractions of the infected cell by immunoprecipitation analysis. The divergent conclusions reached in previous reports as to the subcellular location of the v-*erbA* protein (1, 35, 46) led us to reexamine this issue by use of our v-*erbA*-directed antisera. Our first approach was to attempt to duplicate the subcellular fractionation described by Sap et al. (46), a fractionation scheme reported as yielding a nuclear localization of the v-*erbA* polypeptide. This technique makes use of a low-ionic-strength buffer containing nonionic detergent to lyse the infected cells, followed by a low-speed centrifugation to separate soluble (cytoplasm plus mem-

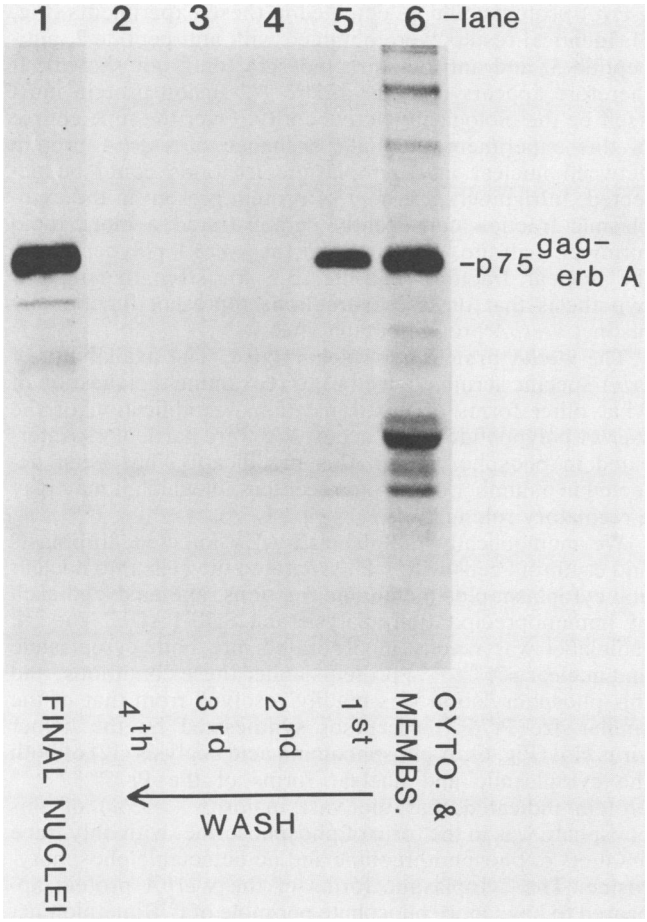

FIG. 3. Subcellular localization of the wild-type v-*erbA* protein by biochemical fractionation. AEV-transformed erythroid cells were radiolabeled with [^{35}S]methionine as described in the text. The cells were then lysed in PTMA buffer, the nuclei were pelleted at 1,000 × *g*, and the supernatant was saved. The nuclear pellet was subsequently washed four times in PTMA buffer, suspended in PTMA buffer–0.5 M NaCl, and sonicated. All fractions were subsequently analyzed by immunoprecipitation with anti-v-*erbA* peptide 2 sera and SDS-PAGE, and the proteins were visualized by fluorography. v-*erbA*-related proteins in the following fractions are shown: the first 1,000 × *g* supernatant, representing the cytoplasm-plus-membrane fraction (lane 6), first nuclear wash (lane 5), second nuclear wash (lane 4), third nuclear wash (lane 3), fourth nuclear wash (lane 2), and final nuclear fraction (lane 1). The position of the 75,000-molecular-weight *gag*-v-*erbA* protein is indicated.

branes) from pelleted (nuclei) fractions. Our initial results confirmed that substantial amounts of the v-*erbA* protein could be recovered in the nuclear fraction by this scheme (data not shown). However, using this procedure on either AEV-infected erythroid or fibroblast cells, we consistently obtained from 40 to 50% of the total v-*erbA* protein in the cytoplasm-plus-membrane fraction (data not shown).

Altering the ionic strength of the lysis buffer had no effect on the observed cytoplasmic/nuclear distribution of the v-*erbA* protein until the NaCl concentration was raised to 400 mM, at which point the nuclei lysed and released the v-*erbA* polypeptide (data not shown). Substituting calcium for magnesium in the lysis buffer also had no observable effect. Substituting phosphate for the Tris in the buffering system did appear to slightly improve our yield of nuclear v-*erbA* protein, but 25 to 35% of the total v-*erbA* protein continued to partition to the nonnuclear fraction even under these optimal conditions (see below).

We next explored whether the v-*erbA* protein found in the cytoplasm-plus-membrane fraction represented a truly separate population of molecules from that found in the nuclear fraction or whether this nonnuclear v-*erbA* protein was due to leakage from the nuclei. We lysed AEV-infected erythroid cells in our optimized lysis buffer, pelleted the nuclei, and then repeatedly washed the nuclei in the same lysis buffer. Each fraction was analyzed for v-*erbA* protein content by immunoprecipitation and SDS-PAGE. After recovery of the initial lysate supernatant (cytoplasm plus membranes; Fig. 3, lane 6) and the first wash (lane 5), repeated washing failed to remove any additional v-*erbA* protein from the nuclei until the final nuclear pellet was disrupted by sonication in a high salt concentration. This result strongly suggests that the v-*erbA* protein released in the cytoplasm-plus-membrane fraction represented a distinct and separate population from that which remained tightly associated with nuclei during the repeated wash steps. We reached a similar conclusion from a related experiment in which isolated nuclei were suspended in lysis buffer and incubated for up to 4 h at 4°C: no v-*erbA* protein leaked out of the nuclei under these conditions.

The validity of our subcellular fractionation scheme was substantiated by assaying our nuclear and cytoplasm-plus-membrane fractions for a number of marker proteins. In our erythroid cell fractionations, 95% of the lactate dehydrogenase activity, a cytoplasmic enzyme marker, was in the cytoplasm-plus-membrane fraction, as was most of the enzymatic activity of markers for endoplasmic reticulum, plasma membrane, Golgi apparatus, and mitochondria (Table 1). Conversely, both histones H5 and 2B, two nuclear markers, partitioned quantitatively into the nuclear fraction under these conditions.

We also applied an alternative subcellular fractionation scheme which relied on Dounce homogenization rather than detergent lysis to break open the AEV-infected cells (13, 40). This procedure was very similar to that of Abrams et al. (1), previously reported to yield an exclusively nonnuclear localization of the v-*erbA* protein. Significant amounts of v-*erbA* protein were found in both the 1,000 × *g* pellet (nuclei) and

TABLE 1. Distribution of marker enzymes in subcellular fractions[a]

Enzyme of protein	Marker for:	Enzyme activity (% total) in fraction[b]:	
		Nuclear	Cytoplasm + membrane
Lactate dehydrogenase	Cytosol	5	95
NADH diaphorase	Endoplasmic reticulum	39	61
Thiamine pyrophosphatase	Golgi apparatus	20	80
5′-Nucleotidase	Plasma membrane	8	92
Succinic reductase	Mitochondria	10	90
Histone H5	Nuclei	100	ND
Histone 2B	Nuclei	100	ND

[a] Enzyme activities were determined as previously described (40). Histone H5 was detected by immunoprecipitation analysis; histone 2B was resolved by SDS-PAGE and visualized by a silver staining technique.

[b] Enzyme activities or protein concentrations (expressed as a percentage of the total) were determined in nonradioactive nuclear and cytoplasm-plus-membrane fractions isolated in parallel to the radiolabeled samples used for the v-*erbA* protein determinations. ND, None detected.

supernatant (cytoplasm plus membranes) by this mechanical homogenization technique, in complete agreement with our results obtained by Triton X-100 lysis (Table 2). Further differential centrifugation of the 1,000 × *g* supernatant fraction revealed that significant amounts of the nonnuclear v-*erbA* protein partitioned as a cytoplasmic polypeptide under these conditions, remaining in the soluble fraction after a 154,000 × *g* centrifugation (Table 2).

Immunofluorescence experiments confirmed that the v-*erbA* protein exists in both nuclear and cytoplasmic forms. An independent elucidation of the subcellular location of the v-*erbA* protein was obtained by the use of indirect immunofluorescence. AEV-infected fibroblasts and fibroblasts infected with a RAV-1 helper virus alone were fixed, permeabilized, and reacted with various primary antisera (Fig. 4). The cells were subsequently reacted with rhodamine-conjugated goat anti-rabbit immunoglobulin and examined under an epifluorescence microscope. Two negative controls, preimmune sera on AEV-infected cells and immune sera on cells infected by the helper virus alone, both produced extremely low backgrounds in these experiments (Fig. 4A and B). Use of v-*erbA*-directed sera on AEV-infected fibroblasts (Fig. 4C) produced a distinct nuclear fluorescence, as well as a somewhat weaker but readily detectable cytoplasmic fluorescence. Nuclear fluorescence obtained with the v-*erbA*-directed sera was consistently excluded from the nucleoli of these cells, and the cytoplasmic fluorescence was diffuse and was not detectably associated with membranes or other organelles. For comparison, AEV-infected cells reacted with a serum directed against the v-*erbB* protein produced a well-defined reticular fluorescence pattern (Fig. 4D), as has been previously described for this membrane-bound oncogene product (26, 47).

The p75 *gag*-v-*erbA* protein does not appear to be proteolytically processed. One goal of our development of v-*erbA*-specific sera was to test whether the *gag* sequences might be proteolytically removed from the $p75^{gag\text{-}erbA}$ protein, releasing a (perhaps functionally active) v-*erbA* fragment which would not have been detected by the *gag*-directed antisera used in previous published experiments. We pulse-labeled AEV-infected erythroid cells for 30 min with [^{35}S]methionine and subjected the labeled cells to various times of chase with unlabeled medium. Despite a slow turnover of the $p75^{gag\text{-}erbA}$ protein, no discrete proteolytic product of the v-*erbA* protein could be detected in these experiments (Fig. 5). Identical results were obtained with anti-peptide 2, anti-peptide 3, and anti-*gag*-directed sera (data not shown). It therefore appears that the $p75^{gag\text{-}erbA}$ fusion protein must itself be the biologically active entity. Over the time course of this experiment, no bulk exchange of v-*erbA* protein between nuclear and cytoplasmic fractions could be detected. Intriguingly, the v-*erbA* protein present in the cytoplasmic fraction consistently demonstrated a more rapid turnover (half-life, 2 h) than did the v-*erbA* polypeptide in the nuclear fraction (half-life, 3.5 h), strengthening our hypothesis that these two fractions represent functionally distinct v-*erbA* protein populations.

TABLE 2. Subcellular fractionation of v-*erbA* protein by mechanical cell lysis

Subcellular fraction[a]	Amt of v-*erbA* protein (arbitrary units)[b]
Purified nuclei	100
Detergent wash of crude nuclei	56
10,000 × *g* pellet	19
154,000 × *g* pellet	7
154,000 × *g* supernatant	23

[a] AEV-transformed erythroid cells were radiolabeled with [^{35}S]methionine for 2 h, washed, lysed by Douce homogenization in a buffer lacking detergents, and fractionated as described previously (40). In brief, crude nuclei were pelleted from the Dounce homogenate at 1,000 × *g*, washed with a detergent buffer, and repelleted. The 1,000 × *g* supernatant was centrifuged first at 10,000 × *g* and then at 154,000 × *g*.

[b] Each fraction was analyzed by immunoprecipitation with v-*erbA*-directed antisera and SDS-PAGE. The gel was fluorographed on X-Omat film (Eastman Kodak Co., Rochester, N.Y.), and the fluorogram was quantitated by using a Hoefer scanning densitometer (care was taken to ensure that all values were within the linear range of the film). The intensity of the v-*erbA* protein band immunoprecipitated from each fraction is presented in arbitrary optical density units.

The v-*erbA* protein is phosphorylated. The availability of *erbA*-specific serum allowed us to reexamine the question of what other forms of posttranslational modification of the v-*erbA* polypeptide might occur. We were particularly interested in phosphorylation: this modification has been detected in a number of steroid receptors, in which it may play a regulatory role (4, 16).

We metabolically radiolabeled AEV-infected fibroblasts and erythroid cells with $^{32}P_i$, separated the cells into nuclear and cytoplasm-plus-membrane fractions, and analyzed each by immunoprecipitation analysis and SDS-PAGE. The ^{32}P radiolabel was readily incorporated into both cytoplasmic and nuclear $p75^{gag\text{-}erbA}$ proteins under these conditions, and this phosphorylation was readily resolved from that of the similar-size $Pr76^{gag}$ precursor synthesized by the helper virus (15) (Fig. 6). A phosphoamino acid analysis (12) of both the cytoplasmic and nuclear forms of the $Pr75^{gag\text{-}v\text{-}erbA}$ protein indicated that the vast majority (>95%) of this phosphate was in the form of phosphoserine, with only trace amounts of phosphothreonine and no detectable phosphotyrosine. The cytoplasmic forms of the v-*erbA* protein appeared to have more phosphate per mole of [^{35}S]methionine-labeled protein than did the nuclear forms when compared in parallel, although the significance of this observation is not clear. In Fig. 6, the ^{32}P-labeled v-*erbA* protein immunoprecipitated with anti-v-*erbA* sera demonstrated a slightly different nuclear/cytoplasmic distribution than did the same protein precipitated with *gag*-directed sera: this was not a reproducible observation, however, and is probably without significance.

The v-*erbA* gene product is a DNA-binding protein. Thyroid hormone receptors are found tightly associated with chromatin and demonstrate the ability to bind to DNA in vitro (3, 33, 37, 53). We asked whether the virally transduced *erbA*-encoded polypeptide retains this DNA-binding property. AEV-infected fibroblasts were radiolabeled with [^{35}S]methionine and lysed (see Materials and Methods). The lysates were incubated with DNA-cellulose, unbound proteins were removed, the DNA-cellulose was washed, and the proteins bound to the DNA-cellulose were eluted with a high salt concentration. The unbound and bound fractions were subsequently analyzed for the presence of $p75^{gag\text{-}erbA}$ by immunoprecipitation with *gag*-directed antisera, followed by SDS-PAGE and autoradiography (Fig. 7). The use of *gag*-directed antisera in this experiment permitted the distribution of the RAV-1 helper virus *gag* proteins to serve as an internal control; identical results were obtained using *erbA*-directed sera (data not shown).

A significant fraction of the v-*erbA* protein bound to the DNA matrix by this method, ranging from 10 to 30% of the total v-*erbA* protein in the cell lysate (Fig. 7, lanes 2 and 5). Inclusion of soluble DNA in the buffer inhibited the binding of the v-*erbA* protein to the DNA-cellulose (lanes 3 and 6),

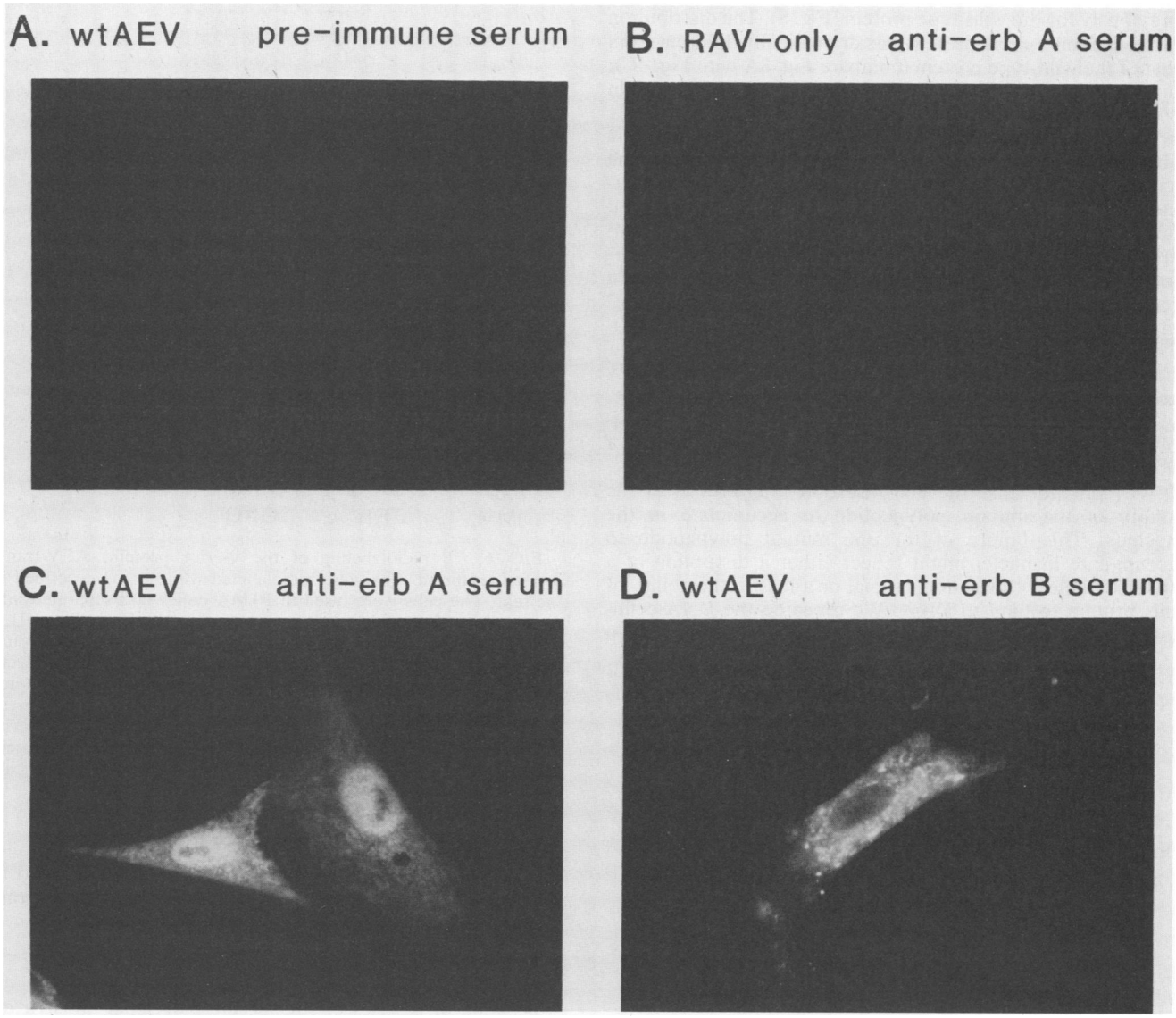

FIG. 4. Immunofluorescence analysis of the subcellular distribution of the wild-type (wt) v-*erbA* protein. Cells were fixed, permeabilized, and reacted with various primary antisera, as described in the text. The cells were subsequently reacted with rhodamine-conjugated goat anti-rabbit immunoglobulin G and photographed by epifluorescence microscopy. Shown are representative microscope fields of fibroblasts infected by RAV helper virus alone and reacted with anti-*erbA* sera (B), fibroblasts infected by AEV and reacted with preimmune sera (A), fibroblasts infected by AEV and reacted with anti-*erbA* sera (C), and fibroblasts infected by AEV and reacted with anti-*erbB* sera (D).

and v-*erbA* protein did not bind to underivatized cellulose (lanes 1 and 4), confirming that the interaction of the v-*erbA* protein was with the DNA moiety. Similar DNA binding was demonstrated by v-*erbA* protein isolated from either the nuclei or cytoplasm of AEV-infected erythroid cells (data not shown). The *gag* proteins encoded by the helper genome, assayed as internal controls, failed to bind to the DNA-cellulose, an additional confirmation of the specificity of this reaction. We do not yet understand why most of the v-*erbA* protein remained in the unbound fraction under these conditions. Perhaps a significant percentage of the v-*erbA* protein was inactivated or denatured during extraction from the cell, or perhaps endogenous nucleic acids present in the cell lysates inhibited binding to the DNA-cellulose. Alternatively, our reaction conditions, derived from a procedure developed for the T3/T4 thyronine receptor (33), may not be optimal for DNA binding by the viral polypeptide.

A mutation introduced into the lysine-arginine codon-rich domain of the v-*erbA* coding sequence inhibits biological activity, DNA binding, and nuclear localization. We have begun a genetic dissection of the v-*erbA* oncogene by the use of site-directed mutagenesis. One of our v-*erbA* mutations, representing an in-frame insertion at position number 366 in the v-*erbA* coding region, disrupted the ability of the v-*erbA* protein to function in potentiating erythroid transformation in an in vitro bone marrow assay (A. Koning, C. Judelson, and M. L. Privalsky, manuscript in preparation). In studying the properties of the polypeptide encoded by this v-*erbA* mutant, we noted that this genetic lesion also appears to have inhibited the ability of this polypeptide to accumulate in the nucleus of the infected cell and to bind to DNA in vitro.

Fibroblasts infected by AEV carrying the 366-mutant form of the v-*erbA* gene were fixed, permeabilized, and subjected to the indirect immunofluorescence technique described

previously for the wild-type protein (Fig. 8). The distribution of the mutant v-*erbA* protein was dramatically different from that of the wild-type protein (compare Fig. 8A with Fig. 4C): the cytoplasmic fluorescence patterns were enhanced in 366-mutant-infected cells, and nuclear forms of the v-*erbA* protein were greatly reduced (Fig. 8A). In contrast to this aberrant distribution of the mutant v-*erbA* polypeptide, the subcellular localization of the v-*erbB* protein in 366-mutant-infected cells was unaltered from that in wild-type-infected fibroblasts (Fig. 8B). The results of biochemical fractionations of 366-mutant-infected fibroblasts were in good agreement with the immunofluorescence data and demonstrated a reduced nuclear accumulation of the mutant $p75^{gag\text{v-}erbA}$ protein relative to the wild-type v-*erbA* protein (Fig. 8C). The amount of v-*erbA* protein remaining in the nuclear fraction of 366-mutant-infected cells, although reproducibly greatly reduced from that of the wild-type polypeptide, varied somewhat from fractionation to fractionation, possibly due to difficulties in obtaining quantitative lysis of fibroblasts adhering to culture plates.

We conclude that the 366 insertion interferes with the ability of the mutant polypeptide to accumulate in the nucleus. This failure of the 366 mutant polypeptide to accumulate in nuclei might reflect either a disruption of a specific nuclear "targeting" signal or a loss in the ability of this protein to bind to DNA. We repeated the DNA-cellulose-binding analysis using v-*erbA* protein isolated from mutant-infected fibroblasts (Fig. 8D). Under our conditions, the $p75^{gag\text{-}erbA}$ protein encoded by the 366 mutant failed to detectably bind to DNA (Fig. 8D, lanes 1 and 3), in contrast to the wild-type v-*erbA* protein assayed in parallel.

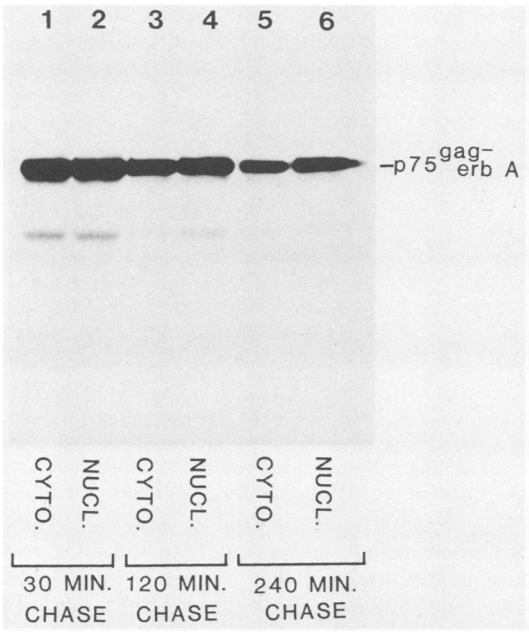

FIG. 5. Pulse-chase analysis of v-*erbA* protein biosynthesis. AEV-transformed erythroid cells were metabolically radiolabeled with [^{35}S]methionine for 30 min at 39°C. The radioisotope was then removed, and the cells were washed and suspended in radiolabel-free complete medium containing 10% fetal bovine serum and 1% chicken serum. The cells were incubated at 39°C for the times indicated, washed with ice-cold PBS, lysed in PTMA buffer, and fractionated into nuclear (lanes 2, 4, and 6) and cytoplasm-plus-membrane (lanes 1, 3, and 5) fractions as described in the text. Each fraction was analyzed by immunoprecipitation with anti-*erbA* sera, and immunoprecipitated proteins were resolved by SDS-PAGE and visualized by fluorography. Shown are the v-*erbA*-related proteins detected after a chase of 30 min (lanes 1 and 2), 120 min (lanes 3 and 4), or 240 min (lanes 5 and 6). The position of the 75,000-molecular-weight (p75) *gag*-v-*erbA* protein is indicated.

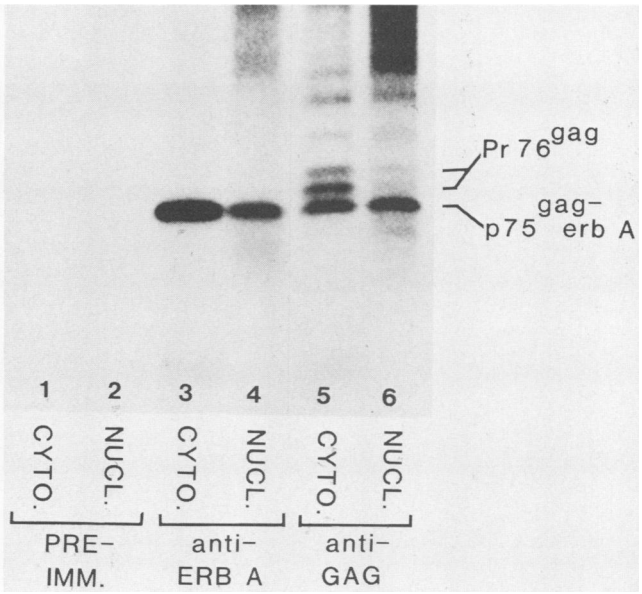

FIG. 6. ^{32}P radiolabeling of the v-*erbA* protein. AEV-transformed erythroid cells were radiolabeled with $^{32}P_i$ as described in the text. The cells were lysed in PTMA buffer and separated into nuclear (lanes 2, 4, and 6) and cytoplasm-plus-membrane (lanes 1, 3, and 5) fractions. Each fraction was analyzed by immunoprecipitation and SDS-PAGE, and the immunoprecipitated proteins were visualized by autoradiography. Shown are the ^{32}P-labeled proteins immunoprecipitated by preimmune sera (lanes 1 and 2), anti-*erbA* sera (lanes 3 and 4), and anti-*gag*-directed sera (lanes 5 and 6). The positions of the 75,000-molecular-weight (p75) *gag*-v-*erbA* protein and the 76,000-molecular-weight (Pr76) *gag* precursor polypeptide are indicated.

DISCUSSION

Isolation of a series of site-specific polyclonal antisera directed against different epitopes within the v-*erbA* protein. Our antisera were raised against chemically synthesized oligopeptides based on the elucidated amino acid sequence of the v-*erbA* protein (14, 46). Antisera prepared against our peptide antigens were capable of highly specific immunoprecipitation of the native $p75^{gag\text{-}erbA}$ protein. Intriguingly, because of an error in the published DNA sequence (14), only 5 of the 10 amino acids in our peptide 3 represent authentic sequence in the v-*erbA* protein (14, 46). Nonetheless, in a limited number of animals peptide 3 elicited immune sera which were capable of (weak) immunoprecipitation of the native $p75^{gag\text{-}erbA}$ protein, in agreement with previous work suggesting the minimal immunological epitope may be quite small (5).

We have been unable to detect the presence of a c-*erbA* protein with our v-*erbA*-directed peptide antisera, although we have only tested a few cell types for c-*erbA* expression (Fig. 2 and unpublished results). Two of our three peptide antigens exactly duplicate the chicken c-*erbA* protein sequence, although both peptides diverge from the two published mammalian c-*erbA* protein sequences (46, 55).

The v-*erbA* protein appears to be present in both cytoplasmic and nuclear forms in AEV-infected cells. An accurate

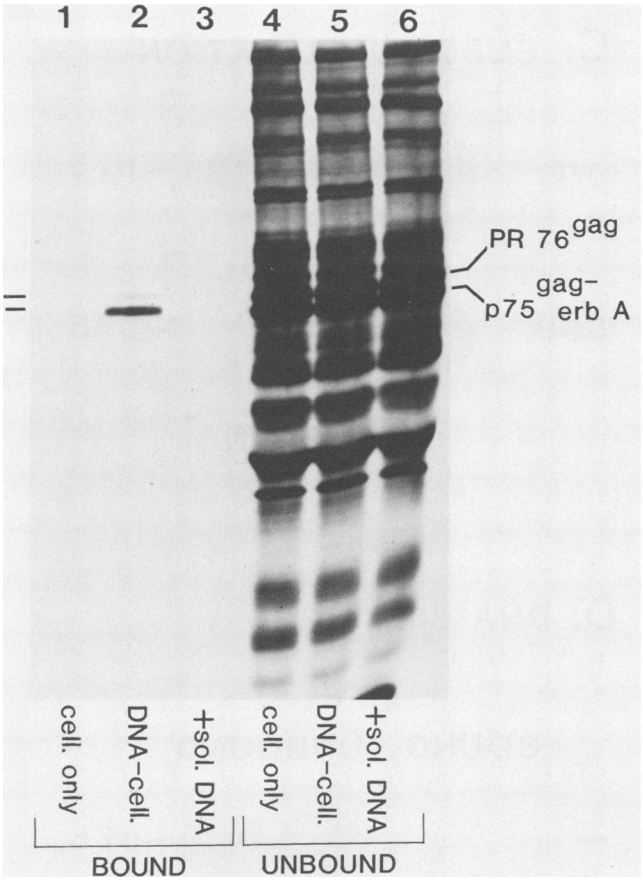

FIG. 7. DNA binding by the v-*erbA* protein. Fibroblasts infected by wild-type AEV were radiolabeled for 2 h with [^{35}S]methionine, washed, and sonicated as described in the text. The cell extracts were then incubated for 1 h at 4°C with either underivatized cellulose (lanes 1 and 4), DNA-cellulose (lanes 2 and 5), or DNA-cellulose in the presence of 2 mg of soluble DNA per ml (lanes 3 and 6), the matrix material was washed, and bound proteins were eluted with a high salt concentration. Proteins that bound to the cellulose or DNA-cellulose (lanes 1 to 3) or failed to bind (lanes 4 to 6) were analyzed by immunoprecipitation by using *gag*-directed antisera, resolved by SDS-PAGE, and visualized by fluorography.

elucidation of the subcellular location of the v-*erbA* protein is essential for establishing a model for the mechanism of action of this oncogenic polypeptide. Early reports, based on a rigorous nuclear isolation procedure, indicated a cytoplasmic localization for the p75$^{gag\text{-}erbA}$ polypeptide, leading to suggestions that the v-*erbA* protein might represent a dysfunctional form of the cellular homolog (1, 10, 35). In this model, the v-*erbA* protein would act by interference, perhaps by blocking transmission of a differentiation signal from the extracellular environment to the functional c-*erbA* mediator (10).

An alternative model, proposed by Sap et al. (46), suggests that the v-*erbA* protein is a nuclear polypeptide and that it might represent a constitutively on derivative of the normal hormonally regulated c-*erbA* protein. This model is consistent with mutagenesis studies performed with steroid hormone receptors, which suggest that deletion of the hormone-binding site results in a receptor molecule constitutively capable of transcriptional activation (20, 22). Sap et al. (46) reported what appears to be an exclusively nuclear localization for the v-*erbA* protein, consistent with this model.

The results of our study are both in agreement and disagreement with these previously published analyses. Using a variety of subcellular fractionation and immunofluorescence techniques, we found that the v-*erbA* protein was clearly present in both nuclear and cytoplasmic fractions of the AEV-infected cell. This apparently dual localization cannot be readily attributed to a general leakage or breakage of nuclei during the fractionation procedure, as demonstrated by our repeated washing experiments, our marker enzyme assays, and our immunofluorescence data. On the other hand, despite the presence of an apparently cytoplasmic form of p75$^{gag\text{-}erbA}$, from 60 to 70% of the v-*erbA* protein in the infected cell does appear to be tightly associated with nuclei by our methods.

We feel that the simplest explanation of our results is that both truly cytoplasmic and nuclear populations of v-*erbA* molecules exist in the infected cell. The function of the cytoplasmic form of the v-*erbA* protein is unclear at this time. Interestingly, cytoplasmic forms of the T3/T4 thyronine receptors have also been reported (for reviews, see references 37 and 53), perhaps representing a functional analogy between the v-*erbA* protein and its putative normal-cell progenitor polypeptide. However, we cannot completely rule out an alternative, although less likely, possibility that two distinct populations of nuclear v-*erbA* protein exist. One population of v-*erbA* protein molecules might be loosely associated with nuclei (perhaps present in the nucleoplasm) and would readily elute from nuclei during detergent-induced or mechanical cell lysis. The second population of v-*erbA* protein molecules might be tightly associated with nuclei, perhaps bound to chromatin, and would therefore be resistant to our washing steps. However, the distinct cytoplasmic fluorescence observed in our v-*erbA*-directed immunofluorescence experiments does not support this alternative possibility.

The reasons for the apparent discrepancies between previously reported subcellular localizations of the v-*erbA* protein (1, 35, 46) probably lie with the relative rigor of the different fractionation protocols. The fractionation procedure of Abrams et al. (1) is relative stringent, involving repeated washes of the nuclei in buffers of differing osmolarity. In attempting to duplicate this procedure, we noted a significant amount of nuclear swelling and lysis toward the final stages of the fractionation, perhaps accounting for the apparent loss of v-*erbA* polypeptide from the nuclei observed in the use of this protocol (1).

The v-*erbA* protein binds to DNA in vitro. The v-*erbA* protein sequence exhibits a structural motif that, in the steroid receptors, is thought to represent a DNA-binding domain (21, 28, 46, 55). This putative DNA-binding domain consists of a cysteine-rich region embedded in a domain high in lysine and arginine residues. A similar cysteine-rich sequence was first identified in transcription factor TFIIIa as a possible zinc-finger domain capable of interacting with DNA (34). If the v-*erbA* protein is functionally analogous to the thyroid and steroid hormone receptors, the retention of DNA-binding activity would be crucial to its mechanism of action as an effector of transcriptional regulation.

We demonstrated that the wild-type v-*erbA* protein isolated from either erythroid or fibroblast host cells and from nuclear or cytoplasmic fractions is able to bind to immobilized DNA in vitro. We presume that this binding assay, using immobilized calf thymus DNA, measures a general affinity of the v-*erbA* protein for DNA or for nucleic acids in general. Both steroid and thyroid hormone receptors demonstrate a similar ability to bind to nontarget DNA se-

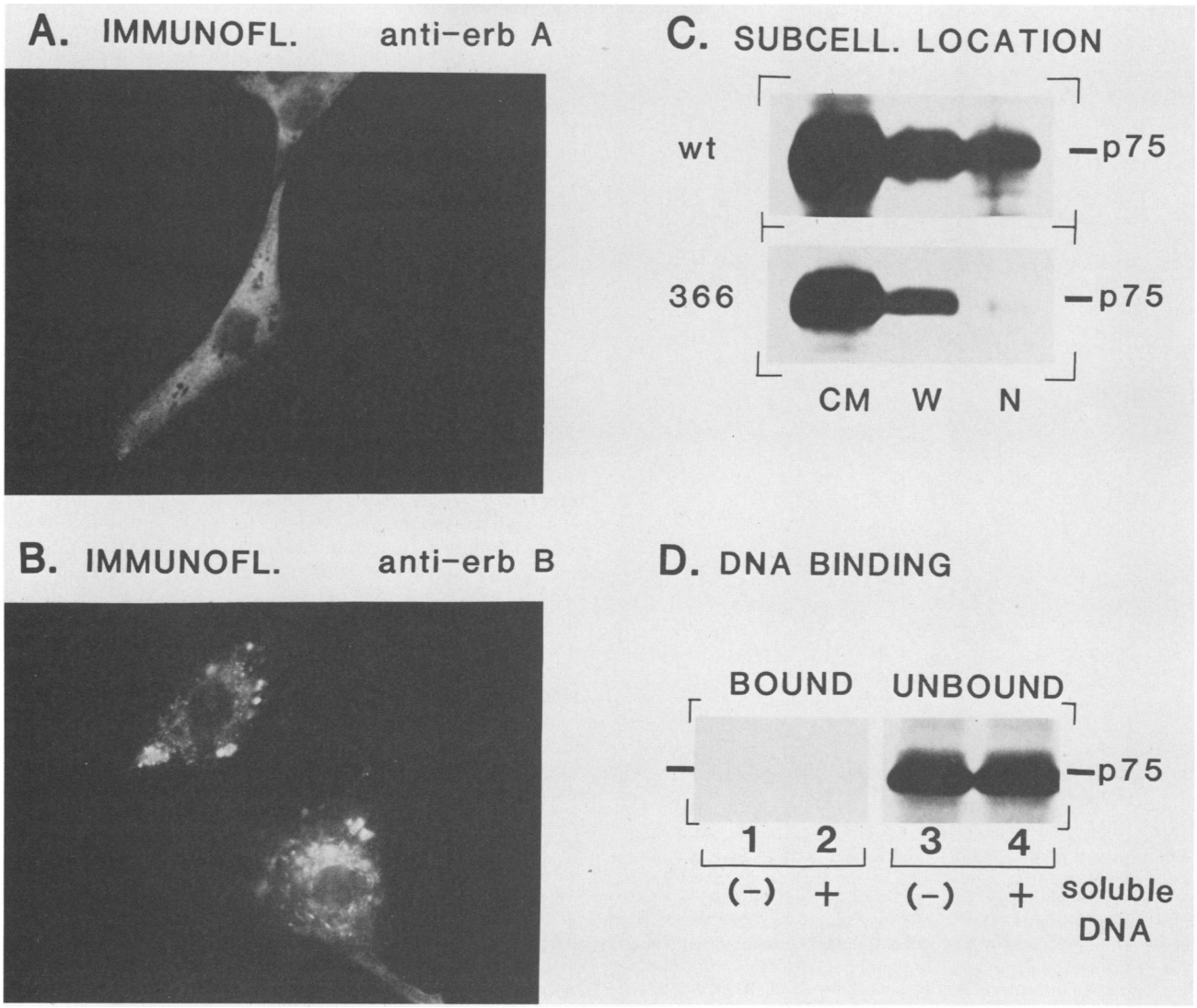

FIG. 8. Analysis of the 366-mutant v-*erbA* protein. The subcellular distribution of the 366-mutant v-*erbA* protein was analyzed by immunofluorescence (A and B) and biochemical fractionation (C), and the ability of the 366-mutant protein to bind to DNA was tested (D). Immunofluorescence analysis of fibroblasts infected by the AEV 366 mutant was performed as described in the legend to Fig. 4, using either anti-v-*erbA* sera (A) or anti-v-*erbB* sera (B); representative epifluorescence photomicrographs are shown. For biochemical fractionation, fibroblasts infected by wild-type AEV or by the 366 mutant were radiolabeled with [^{35}S]methionine, lysed in PTMA buffer containing 50 mM phosphate, and separated into different subcellular fractions as described in the text; wild-type (wt) and mutant 366 forms were assayed in parallel. The distribution of these p75$^{gag\text{-}v\text{-}erbA}$ proteins in cytoplasm-plus-membrane (CM), wash (W), and final nuclear pellet (N) fractions is shown (C). The ability of the 366-mutant v-*erbA* protein to bind to DNA-cellulose (D) was tested as described in the legend to Fig. 7. The p75$^{gag\text{-}v\text{-}erbA}$ protein that bound (lanes 1 and 2) or failed to bind (lanes 3 and 4) to the DNA-cellulose is shown. The experiment was performed in the absence (lanes 1 and 3) or presence (lanes 2 and 4) of 2 mg of soluble DNA per ml as a competitor.

quences. In addition, specific enhancerlike DNA sequences which mediate the interaction of steroid receptors with their target genes have been characterized (for a review, see reference 56). We are currently attempting to identify similar specific DNA-binding sites for the v-*erbA* polypeptide, using probes derived from T3/T4 thyronine-regulated genes.

A lysine-arginine-rich domain within the v-*erbA* protein may represent a nuclear localization signal or DNA-binding sequence or both. We engineered an insertion mutation into the v-*erbA* coding sequence which introduced an in-frame *Hpa*I oligonucleotide linker (GTTAAC) into the DNA at position 366. This insertion, introducing a valine-asparagine codon pair, abolishes the ability of the v-*erbA* protein to potentiate erythroid transformation (unpublished data). In parallel, the mutant v-*erbA* protein, although synthesized at wild-type levels, appears to be partially or fully defective in the ability to accumulate in the nucleus of infected fibroblasts. In addition, this mutant polypeptide fails to bind to DNA in vitro. It is likely that the disruption in these biochemical functions, DNA binding and nuclear localization, are responsible for the biological defect of the 366 insertion mutant. However, this conclusion must be applied cautiously, for the overall effects of this genetic lesion on the conformation and function of the v-*erbA* polypeptide are unknown.

It is possible that nuclear localization of the wild-type v-*erbA* protein is due simply to the affinity it has for DNA or chromatin or both and that the 366 mutation, by disrupting

(126)	-Pro Pro Lys Lys Lys Arg Lys Val-	SV-40 T ag
(279)	-Pro Pro Lys Lys Ala Arg Glu Asp-	Polyoma T ag 1
(189)	-Val Ser Arg Lys Arg Pro Arg Pro-	Polyoma T ag 2
(118)	-Val Ala Lys Arg Lys*Leu Ile Glu-	v-erb A 1
(128)	-Arg Glu Arg Arg Arg Lys Glu Glu-	v-erb A 2

FIG. 9. Potential nuclear localization signals in the v-*erbA* protein sequence. Two regions within the v-*erbA* protein sequence proximal to the 366 mutation are shown (v-*erbA*1 and v-*erbA*2) and compared with known nuclear localization signals present in the simian virus 40 and polyomavirus large-T antigens (T ag) (44). The polyomavirus T antigen contains two distinct signal sequences. Regions of amino acid similarity are boxed. The numbers in parentheses refer to the position (in codons) of each sequence from the start of the corresponding polypeptide. The asterisk represents the site in the v-*erbA* protein corresponding to the 366 insertion mutation (at 366 base pairs, after codon 122).

DNA binding, also prevents nuclear accumulation. However, an alternative explanation is that the position 366 insertion has disrupted a nuclear localization target sequence, as well as the DNA-binding domain itself. Intriguingly, the sequence disrupted by the 366 mutant has a strong similarity to nuclear localization signals found in the simian virus 40 and polyomavirus large-T antigens (Fig. 9). A common motif in the T-antigen molecules, shared by the v-*erbA* protein sequence, is a strong preponderance of highly basic amino acids. It has been demonstrated for both simian virus 40 and polyomavirus large-T antigens that these nuclear localization signals can be distinct from sequences mediating DNA binding. We are attempting to further define these functions in v-*erbA* by the analysis of additional site-specific mutations.

Our results are therefore largely in agreement with a model of the v-*erbA* protein functioning in oncogenesis as a constitutively on derivative of a hormone receptor, presumably acting by modulating transcription of specific target genes within the nucleus of the transformed erythroid cell (46). This premise is consistent with data obtained with the steroid hormone receptors, in which deletion of the hormone-binding domain leads to a receptor capable of the constitutive activation of transcription of target genes (21, 28). In common with these engineered steroid receptor mutants, the wild-type v-*erbA* protein appears to have lost the ability to bind hormone ligand (46). However, more experiments will need to be performed to fully rule out possible alternative mechanisms of v-*erbA* protein action.

ACKNOWLEDGMENTS

We thank Cathy Judelson for superb technical assistance, Steven Palmieri for helpful discussions, and all of the members of the Department of Bacteriology, University of California, Davis, for generous encouragement and support.

This work was supported by Public Health Service grant CA38823 from the National Institutes of Health. P.B. was supported, in part, by the University of California, Davis, Research Mentorship Program.

ADDENDUM

After this article was submitted, D. Picard and K. R. Yamamoto (EMBO J. **6**:3333–3340, 1987) reported the identification of a nuclear localization signal in the glucocorticoid receptor with a similar sequence and in a position equivalent to the site of our 366 insertional mutant within the v-*erbA* protein.

LITERATURE CITED

1. **Abrams, H. D., L. R. Rohrschneider, and R. N. Eisenman.** 1982. Nuclear localization of the putative transforming protein of avian myelocytomatosis virus. Cell **29**:427–439.
2. **Anderson, S. M., W. S. Hayward, B. G. Neel, and H. Hanafusa.** 1980. Avian erythroblastosis virus produces two mRNA's. J. Virol. **36**:676–683.
3. **Apriletti, J., Y. Davis-Inouye, J. D. Baxter, and N. Eberhardt.** 1983. Physiochemical characterization of the intranuclear thyroid hormone receptor, p. 67–97. *In* J. H. Oppenheimer and H. E. Samuels (ed.), Molecular basis of thyroid hormone action. Academic Press, Inc., New York.
4. **Aurichhio, F., A. Miliaccio, A. Rotondi, and G. Castoria.** 1985. Phosphorylation on tyrosine of the estradiol receptor, p. 279–298. *In* V. K. Moudgill (ed.), Molecular mechanisms of steroid hormone action. Walter de Gruyter, Inc., New York.
5. **Barlow, D. J., M. S. Edwards, and J. M. Thornton.** 1986. Continuous and discontinuous antigenic determinants. Nature (London) **322**:747–748.
6. **Beug, H., T. Graf, and M. J. Hayman.** 1981. Production and characterization of antisera specific for the *erb* protein of p75, the presumptive transforming protein of avian erythroblastosis virus. Virology **111**:201–210.
7. **Beug, H., M. J. Hayman, M. B. Raines, H. J. Kung, and B. Vennström.** 1986. Rous-associated virus 1-induced erythroleukemic cells exhibit a weakly transformed phenotype in vitro and release c-*erbB*-containing retroviruses unable to transform fibroblasts. J. Virol. **57**:1127–1138.
8. **Beug, H., S. Palmieri, C. Freudenstein, H. Zentgraf, and T. Graf.** 1982. Hormone dependent terminal differentiation *in vitro* of chicken erythroleukemic cells transformed by ts mutants of avian erythroblastosis virus. Cell **28**:907–919.
9. **Beug, H., A. von Kirchbach, G. Doderlein, J. F. Conscience, and T. Graf.** 1979. Chicken hematopoietic cells transformed by seven strains of defective leukemia viruses display three distinct phenotypes of differentiation. Cell **18**:375–390.
10. **Bishop, J. M.** 1986. Oncogenes as hormone receptors. Nature (London) **321**:112–113.
11. **Conneely, O. M., W. P. Sullivan, D. O. Toft, M. Birbaumer, R. G. Cook, B. L. Maxwell, T. Zarucki-Schulz, G. L. Greene, W. T. Schrader, and B. W. O'Malley.** 1986. Molecular cloning of the chicken progesterone receptor. Science **233**:767–770.
12. **Cooper, J. A., B. M. Sefton, and T. Hunter.** 1983. Detection and quantification of phosphotyrosine in proteins. Methods Enzymol. **99**:387–402.
13. **Courtneidge, S. A., A. D. Levinson, and J. M. Bishop.** 1980. The protein encoded by the transforming gene of avian sarcoma virus ($p60^{src}$) and a homologous protein in normal cells ($p60^{proto\text{-}src}$) are associated with the plasma membrane. Proc. Natl. Acad. Sci. USA **77**:3783–3787.
14. **DeBuire, B., C. Henry, M. Benaissa, G. Biserte, J. M. Claverie, S. Saule, P. Martin, and D. Stehelin.** 1984. Sequencing the *erb* A gene of avian erythroblastosis virus reveals a new type of oncogene. Science **224**:1456–1459.
15. **Dickson, C., R. Eisenman, H. Fan, E. Hunter, and N. Teich.** 1984. Protein biosynthesis and assembly, p. 513–648. *In* R. Weiss, N. Teich, H. Varmus, and J. Coffin (ed.), RNA Tumor Viruses, 2nd ed. Cold Spring Harbor Laboratory, Cold Spring Harbor, N.Y.
16. **Dougherty, J. J.** 1985. Phosphorylation of the progesterone receptor, p. 279–298. *In* V. K. Moudgill (ed.), Molecular mechanisms of steroid hormone action. Walter de Gruyter, Inc., New York.
17. **Frykberg, L., S. Palmieri, H. Beug, T. Graf, M. J. Hayman, and B. Vennstrom.** 1983. Transforming capacities of avian erythroblastosis virus mutants deleted in the *erb* A or B oncogenes. Cell **32**:227–238.
18. **Gandrillon, O., P. Jurdic, M. Benchaibi, J.-H. Xiao, J. Ghysdael, and J. Samarut.** 1987. Expression of the v-*erb* A oncogene in chicken embryo fibroblasts stimulates their proliferation *in vitro* and enhances tumor formation *in vivo*. Cell **49**:687–697.
19. **Gazzolo, L., C. Moscovici, G. Moscovici, and J. Samarut.** 1979. Response of hematopoietic cells to avian acute leukemia vi-

ruses: effect on the differentiation of the target cells. Cell **16:** 627–638.
20. **Gilmore, T., J. E. DeClue, and G. S. Martin.** 1985. Protein phosphorylation at tyrosine is induced by the v-*erb* B gene product *in vivo* and *in vitro*. Cell **40:**609–618.
21. **Godowski, P. J., S. Rusconi, R. Miesfeld, and K. R. Yamamoto.** 1987. Glucocorticoid receptor mutants that are constitutive activators of transcriptional enhancement. Nature (London) **325:**365–368.
22. **Graf, T., and H. Beug.** 1983. Role of the v-*erb* A and v-*erb* B oncogenes of avian erythroblastosis virus in erythroid cell transformation. Cell **34:**7–9.
23. **Graf, T., A. von Kirchbach, and H. Beug.** 1981. Characterization of the hematopoietic target cells of AEV, MC-29, and AMV avian leukemia viruses. Exp. Cell Res. **131:**331–343.
24. **Green, S., P. Walter, V. Kumar, A. Krust, J. M. Bornet, P. Argos, and P. Chambon.** 1986. Human oestrogen receptor cDNA: sequence, expression, and homology to v-*erb* A. Nature (London) **320:**134–139.
25. **Greene, G. L., P. Gilna, M. Waterfield, A. Baker, Y. Hort, and J. Shine.** 1986. Sequence and expression of human estrogen receptor complementary DNA. Science **231:**1150–1154.
26. **Hayman, M. J., G. Ramsey, K. Savin, G. Kitchner, T. Graf, and H. Beug.** 1983. Identification and characterization of the avian erythroblastosis virus *erb* B gene product as a membrane glycoprotein. Cell **32:**579–588.
27. **Hayman, M. J., B. Royer-Pokora, and T. Graf.** 1979. Defectiveness of avian erythroblastosis virus: synthesis of a 75K *gag*-related protein. Virology **92:**31–45.
28. **Hollenberg, S. M., V. Giguerre, P. Segui, and R. M. Evans.** 1987. Colocalization of DNA-binding and transcriptional activation functions in the human glucocorticoid receptor. Cell **49:**39–46.
29. **Kahn, P., L. Frykberg, C. Brady, I. Stanley, H. Beug, B. Vennstrom, and T. Graf.** 1986. v-*erb* A cooperates with sarcoma oncogenes in leukemia cell transformation. Cell **45:**349–356.
30. **Kitchener, G., and M. J. Hayman.** 1980. Comparative tryptic peptide mapping studies suggest a role in cell transformation for the *gag*-related proteins of avian erythroblastosis virus and the myelocytomatosis viruses CMII and MC-29. Proc. Natl. Acad. Sci. USA **77:**1637–1641.
31. **Kris, R. M., I. Lax, W. Gullick, M. D. Waterfield, A. Ullrich, M. Fridkin, and J. Schlessinger.** 1985. Antibodies against a synthetic peptide as a probe for the kinase activity of the avian EGF-receptor and v-*erb* B proteins. Cell **40:**619–625.
32. **Lai, M. M. C., J. C. Neil, and P. K. Vogt.** 1980. Cell-free translation of avian erythroblastosis virus RNA yields two specific and distinct proteins with molecular weights of 75,000 and 40,000. Virology **100:**475–483.
33. **MacLeod, K. M., and J. D. Baxter.** 1976. Chromatin receptors for thyroid hormones. J. Biol. Chem. **251:**7380–7387.
34. **Miller, J., A. D. MacLachlan, and A. Klug.** 1985. Repetitive zinc-binding domains in the protein transcription factor IIIA from Xenopus oocytes. EMBO J. **4:**1609–1617.
35. **Moelling, K. M., K. Owada, I. Greiser-Wilke, T. Bunte, and P. Donner.** 1982. Biochemical characterization of transformation specific proteins of acute avian leukemia and sarcoma viruses. J. Cell. Biochem. **20:**63–69.
36. **Ng, M., and M. L. Privalsky.** 1986. Structural domains of the avian erythroblastosis virus *erbB* protein required for fibroblast transformation: dissection by in-frame insertional mutagenesis. J. Virol. **58:**542–553.
37. **Oppenheimer, J. H.** 1983. The nuclear receptor-triiodothyronine complex: relationship to thyroid hormone distribution, metabolism, and biological activity, p. 1–35. *In* J. H. Oppenheimer and H. H. Samuels (ed.), Molecular basis of thyroid hormone action. Academic Press, New York.
38. **Pawson, T., and G. S. Martin.** 1980. Cell-free translation of avian erythroblastosis virus RNA. J. Virol. **34:**280–284.
39. **Privalsky, M. L., and J. M. Bishop.** 1982. Proteins specified by avian erythroblastosis virus: coding region localization and identification of a previously undetected *erb* B polypeptide. Proc. Natl. Acad. Sci. USA **79:**3958–3963.
40. **Privalsky, M. L., and J. M. Bishop.** 1984. Subcellular localization of the v-*erb* B protein, the product of a transforming gene of avian erythroblastosis virus. Virology **135:**356–368.
41. **Privalsky, M. L., R. Ralston, and J. M. Bishop.** 1984. The membrane glycoprotein encoded by the retroviral oncogene v-*erb* B is structurally related to tyrosine-specific protein kinases. Proc. Natl. Acad. Sci. USA **81:**704–707.
42. **Privalsky, M. L., L. Sealy, J. M. Bishop, J. P. McGrath, and A. D. Levinson.** 1983. The product of the avian erythroblastosis virus *erb* B locus is a glycoprotein. Cell **32:**1257–1267.
43. **Rettenmier, C. W., S. M. Anderson, M. W. Rieman, and H. Hanafusa.** 1979. *gag*-related polypeptides encoded by replication-defective avian oncoviruses. J. Virol. **32:**749–761.
44. **Richardson, W. D., B. L. Roberts, and A. E. Smith.** 1986. Nuclear localization signals in polyoma virus large T. Cell **44:**77–85.
45. **Samarut, J., and L. Gazzolo.** 1982. Target cells infected by avian erythroblastosis virus differentiate and become transformed. Cell **28:**921–929.
46. **Sap, J., A. Munoz, K. Damm, Y. Goldberg, J. Ghysdael, A. Leutz, H. Beug, and B. Vennstrom.** 1986. The *erb* A protein is a high affinity receptor for thyroid hormone. Nature (London) **324:**635–640.
47. **Schatzman, R. C., G. I. Evan, M. L. Privalsky, and J. M. Bishop.** 1986. Orientation of the v-*erb*-B gene product in the plasma membrane. Mol. Cell. Biol. **6:**1329–1333.
48. **Schrier, M., G. Koher, H. Hengartner, C. Berek, M. Truco, L. Forni, T. Staehelin, J. Sticker, and B. Takacs.** 1980. Hybridoma Techniques, p. 23–25. Cold Spring Harbor Laboratory, Cold Spring Harbor, N.Y.
49. **Sealy, L., G. Moscovici, C. Moscovici, and J. M. Bishop.** 1983. Site-specific mutagenesis of avian erythroblastosis virus: v-*erb* A is not required for transformation of fibroblasts. Virology **130:**179–194.
50. **Sealy, L., M. L. Privalsky, G. Moscovici, C. Moscovici, and J. M. Bishop.** 1983. Site-specific mutagenesis of avian erythroblastosis virus: v-*erb* B is required for oncogenicity. Virology **130:**155–177.
51. **Sheiness, D., B. Vennstrom, and J. M. Bishop.** 1981. Virus-specific RNAs in cells infected by avian myelocytomatosis virus and avian erythroblastosis virus: modes of oncogene expression. Cell **23:**291–300.
52. **Tainer, J. A., E. D. Getzoff, Y. Paterson, A. Olsen, and R. A. Lerner.** 1985. The atomic mobility component of protein antigenicity. Annu. Rev. Immunol. **3:**501–535.
53. **Tata, J. H.** 1980. Thyroid hormone receptors, p. 127–146. *In* D. Schulster and A. Levitzki (ed.), Cellular receptors for hormones and neurotransmitters. John Wiley & Sons, Inc., New York.
54. **Weinberger, C., S. M. Hollenberg, M. G. Rosenfeld, and R. M. Evans.** 1985. Domain structure of human glucocorticoid receptor and its relationship to the v-*erb* A oncogene product. Nature (London) **318:**670–672.
55. **Weinberger, C., C. C. Thompson, E. S. Ong, R. Lebo, D. J. Gruol, and R. M. Evans.** 1986. The c-*erb* A gene encodes a thyroid hormone receptor. Nature (London) **324:**641–646.
56. **Yamamoto, K. R.** 1985. Steroid receptor regulated transcription of specific genes and gene networks. Annu. Rev. Genet. **19:** 209–252.
57. **Yamamoto, T., Y. Nishida, N. Miyajimi, S. Kawai, T. Ooi, and K. Toyoshima.** 1983. The *erb* B gene of avian erythroblastosis virus is a member of the *src* gene family. Cell **35:**71–78.
58. **Yoshida, M., and K. Toyoshima.** 1980. *In vitro* translation of avian erythroblastosis virus RNA: identification of two major polypeptides. Virology **100:**484–487.